# Quantum, classical and semiclassical momentum distributions. II. Morse and Coulomb potential

**H J Korsch‡ and B Schellhaaß**

FB Physik, Universität, 67653 Kaiserslautern, Germany

**Abstract.** The basic properties of momentum distributions in quantum mechanics for elementary systems as well as their (semi-)classical analogue derived in a preceding paper, are illustrated by a detailed analysis of the Morse oscillator and the three–dimensional Coulomb potential, where the distributions can be calculated in closed form.

## 1. Introduction

Momentum distributions in classical and quantum systems may be useful to study the basic properties of quantum systems. In a preceding paper [1] (in the following denoted as paper I) we discussed the basic properties of momentum distributions as well as the semiclassical approximation, which relates the quantum world to the classical one. Some elementary examples of one–dimensional bound–state systems have also been discussed. In the present article we will illustrate the basic features of the momentum distributions by a detailed discussion of two examples, which allow a calculation in closed form. The first one is a special anharmonic oscillator in one dimension, the Morse potential, which is often used to model molecular vibrations. It is demonstrated that the quantum momentum distributions have for a non–symmetric potential *no* zeros and are almost classical for high energies. The second example is the three–dimensional Coulomb potential, which has important applications in atomic physics. Here the classical and quantum momentum distributions appear to be simpler than the results in coordinate space: The classical orbits in momentum space are, e.g., simple circles.

## 2. Morse potential

One of the often addressed examples of an anharmonic oscillator is the Morse potential

$$V(q) = D\big(1 - e^{-aq}\big)^2 , \tag{2.1}$$

where $D$ is the dissociation energy. For small $q$ we find $V(q) \approx D(aq/2)^2 = m\omega^2 q^2/2$ with $\omega = a\sqrt{2D/m}$. We use the natural units of this harmonic oscillator, i.e. we use

‡ korsch@physik.uni-kl.de

energys in units of $\hbar\omega$ and length units $\sqrt{\hbar/m\omega}$. In these dimensionless variables, $m$ and $\hbar$ are unity and $a$ and $D$ are related by $a = 1/\sqrt{2D}$.

The Morse oscillator is an exceptional case, because a closed form solution exists [2] with energy eigenvalues

$$E_n = n + \frac{1}{2} - \frac{1}{4D}\left(n + \frac{1}{2}\right)^2 ; \qquad n = 0,\, 1,\, \ldots\,,\, n_{max} \tag{2.2}$$

with $n_{max} \leq 2D + 1/2$, i.e. there exist only a finite number of bound states. The term formula reduces to the harmonic oscillator eigenvalues for $n \ll 2D + 1/2$. In order to simplify the notation we introduce the abbreviations $y = 4D\exp(-aq)$ and $s_n = 2D - n - 1/2$. The wavefunctions can be written in terms of confluent hypergeometric functions ${}_1F_1$ as

$$\phi_n(q) = A_n\, \mathrm{e}^{-y/2}\, {}_1F_1(-n, 2s_n + 1; y) = A_n\, \mathrm{e}^{-y/2} \sum_{j=0}^{n} \frac{(-n)_j y^j}{(2s_n + 1)_j j!}\,, \tag{2.3}$$

where $(y)_n = y(y+1)\cdots(y+n-1)$ is the Pochhammer symbol [3] and the normalization constant is

$$A_n = (2s_n + 1)_n \sqrt{\frac{2as_n}{n!\Gamma(4D - n)}}\,. \tag{2.4}$$

The momentum distribution, i.e. the Fourier transform of $\Phi_n(q)$ ((2.3) in paper I) is [4, 5]

$$\begin{aligned}
\psi_n(p) &= \big(4D\big)^{-\mathrm{i}p/a} \frac{A_n}{a\sqrt{\pi}} \int_0^\infty \mathrm{e}^{-y/2}\, y^{s_n + \mathrm{i}p/a - 1}\, {}_1F_1(-n, 2s_n + 1; y)\, \mathrm{d}y \\
&= \big(4D\big)^{-\mathrm{i}p/a} \frac{A_n}{a\sqrt{\pi}}\, 2^{s_n}\Gamma(s_n + \mathrm{i}p/a)\, {}_2F_1(-n, s_n + \mathrm{i}p/a; 2s_n + 1; 2) \\
&= \big(4D\big)^{-\mathrm{i}p/a} \frac{A_n}{a\sqrt{\pi}}\, 2^{s_n}\Gamma(s_n + \mathrm{i}p/a) \sum_{j=0}^{n} \frac{(-n)_j (s_n + \mathrm{i}p/a)_j 2^j}{(2s_n + 1)_j j!}
\end{aligned} \tag{2.5}$$

(see integral 3.2.16 in [6]), where ${}_2F_1$ is a hypergeometric function.

The classical and semiclassical momentum distributions can also be calculated in closed form. First, from equation (2.7) in paper I the period of oscillation is evaluated as

$$T = \frac{2\pi}{\sqrt{1 - E/D}}. \tag{2.6}$$

With the abbreviation

$$z = \sqrt{1 - \frac{p^2}{2E}} \tag{2.7}$$

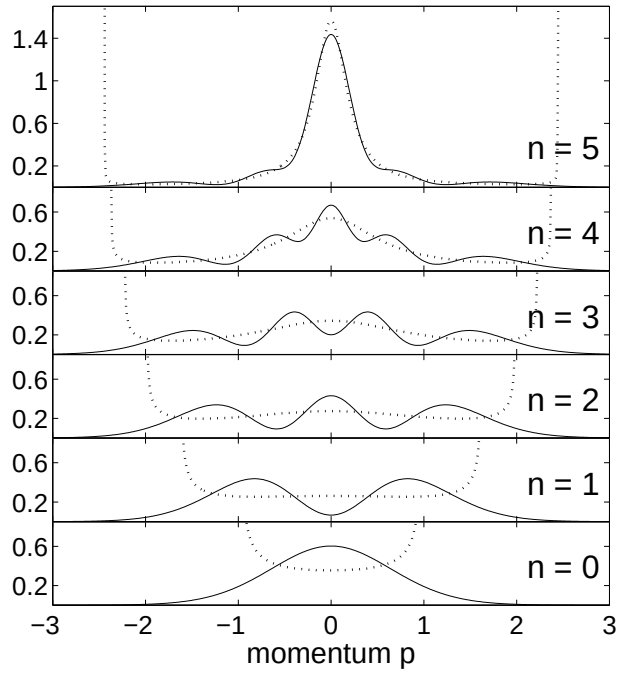


**Figure 1.** *Quantum (line) and classical (dotted) momentum distributions for a Morse oscillator with $D = 3$.*

and $E = p^2/2 + D(1 - \exp(-aq))^2$ the two branches of the $p \longleftrightarrow q$ mapping are given by $aq_\pm = -\ln(1 \mp z\sqrt{E/D})$. The two contributions to the momentum distribution are

$$A_\pm^2(p) = \left(T \left|\frac{\mathrm{d}V}{\mathrm{d}q}\right|_\pm\right)^{-1} = \frac{\sqrt{1 - E/D}}{2\pi z\sqrt{2E}(1 \mp z\sqrt{E/D})} \tag{2.8}$$

and the purely classical distribution is the sum of both contributions

$$w_n(p) = A_+^2 + A_-^2 = \frac{\sqrt{1 - E/D}}{\pi z\sqrt{2E}(1 - z^2E/D)} = \frac{2}{\pi}\frac{\sqrt{D}(D - E)}{[2(D - E) + p^2]\sqrt{2E - p^2}} \tag{2.9}$$

(see also [7]). It is important to realize that because of the assymetry of the potential the two contributions from $q_+ > 0$ and $q_- < 0$ have different weights. For higher energies the momentum distribution is dominated by the contribution from $q_+$, where the potential is flat and the particle spends a much longer time in the interval $[p\,,\, p + dp]$ (compare figure 1 in paper I). This leads to a pronounced peak in the momentum distributions at small $p$ values, where the distribution is almost entirely determined by the $q_+$ term.

As an example, the quantum and classical momentum distributions for a Morse oscillator with $D = 3$ (six bound states) are shown in figure 1 (see also [4]). We observe, that the quantum number $n$ is still reflected in the number of oscillations. However, the momentum wavefunctions have *no* zeros and, with increasing energy, the distributions become more and more classical due to the decreasing importance of the interference with the small contribution from the steep repulsive part of the potential.

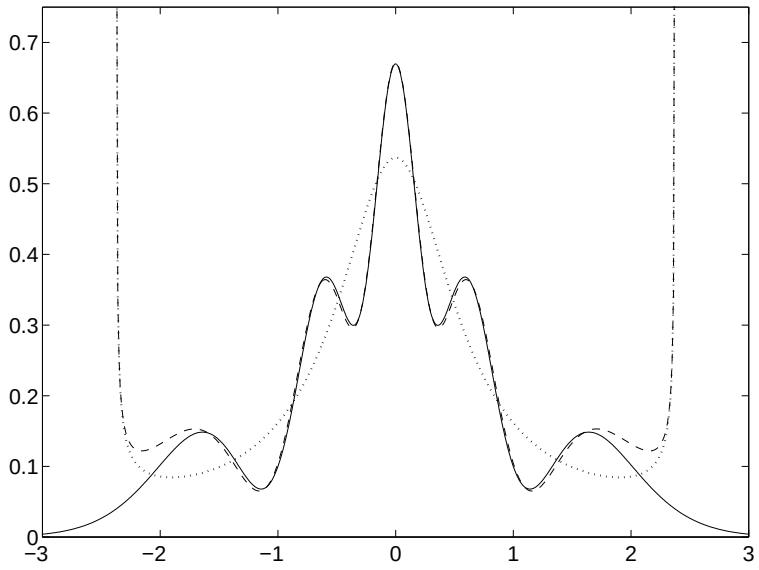


**Figure 2.** *Quantum (line), classical (dotted) and semiclassical (dashed) momentum distributions for the state $n = 4$ of a Morse oscillator with $D = 3$.*

Finally we will evaluate the action integrals and the semiclassical momentum wavefunction. The actions in momentum space are

$$\begin{aligned} S_\pm(p) &= \int_0^p q_\pm(p', E)\,\mathrm{d}p' \\ &= 2\sqrt{D}\left[\sqrt{E(1-z^2)}\left(1 - \ln\left(1 \mp z\sqrt{E/D}\right) \pm \sqrt{D}\left(\frac{\pi}{2} - \arcsin z\right)\right.\right. \\ &\quad \left.\left. + \sqrt{D-E}\left(\mp\frac{\pi}{2} - \arcsin\frac{\mp z + \sqrt{E/D}}{1 \mp z\sqrt{E/D}}\right)\right] \end{aligned} \tag{2.10}$$

and the action difference is given by

$$\begin{aligned} S_+(p) - S_-(p) = 2\sqrt{D}\Bigg[&\sqrt{D}\big(\pi - 2\arcsin z\big) + \sqrt{E(1-z^2)}\ln\frac{1 + z\sqrt{E/D}}{1 - z\sqrt{E/D}} \\ &- \sqrt{D-E}\left(\pi + \arcsin\frac{-z + \sqrt{E/D}}{1 - z\sqrt{E/D}} - \arcsin\frac{z + \sqrt{E/D}}{1 + z\sqrt{E/D}}\right)\Bigg]. \end{aligned} \tag{2.11}$$

As demonstrated in figure 2 for the state $n = 4$, the semiclassical wavefunctions

$$|\psi_E(p)|^2 \approx A_+^2(p) + A_-^2(p) + 2A_+(p)A_-(p)\cos\left[\Delta S(p)/\hbar + \pi/2\right] \tag{2.12}$$

are in close agreement with the quantum ones, except, of course, in the classical turning point region.

As a last remark, we observe that for $p = 0$ the interference is always constructive for even values of $n$ and destructive for odd values as explained in the semiclassical analysis above.

27 October 1999

## 3. Coulomb potential

As an example in three space dimensions we will evaluate the momentum distributions for the bound states of the attractive Coulomb potential

$$V(r) = -\frac{c}{r}, \quad c > 0\,. \tag{3.1}$$

The reader should be well aware of the fact, that this case is, despite of its importance in atomic physics, not at all typical. On the contrary, the Coulomb potential shows many unique properties, which simplify the dynamics. Let us only note that a generic three dimensional potential generates mixed regular/chaotic classical dynamics and a semiclassical analysis is extremely difficult (see, e.g., [8]). If we restrict ourselves to spherically symmetric potentials, the dynamics is integrable and the analysis simpler. The Coulomb potential is, however, still not typical in this class, because all its bound classical orbits are closed curves. This property is only shared with the three–dimensional harmonic oscillator. The period of the orbits with an energy

$$E = \frac{p^2}{2m} - \frac{c}{r} < 0 \tag{3.2}$$

and an angular momentum $\vec{L}$ is

$$T = \pi c \sqrt{\frac{m}{2|E|^3}}\,, \tag{3.3}$$

where $m$ is the (reduced) mass. This period is independent of the angular momentum. Moreover, the Coulomb potential possesses an additional constant of motion the Hermann–Bernoulli–Laplace vector

$$\vec{A} = \vec{p} \times \vec{L} - mc\,\hat{r}\,, \tag{3.4}$$

which is often denoted as the Runge–Lenz vector (for a discussion of the prehistory of this vector see [9, 10]). Note that $\vec{A}$ is orthogonal to the angular momentum $\vec{L}$, i.e. it is a vector in the plane of the orbit. This constant of motion can be easily used to derive the elliptic orbits in position space and — even more easily — to show that the orbits in momentum space are circles

$$(\vec{p} - \vec{p}_0)^2 = \rho^2 \tag{3.5}$$

where the radius

$$\rho = \frac{mc}{L} \tag{3.6}$$

and the center

$$\vec{p}_0 = \frac{\vec{L} \times \vec{A}}{L^2} \tag{3.7}$$

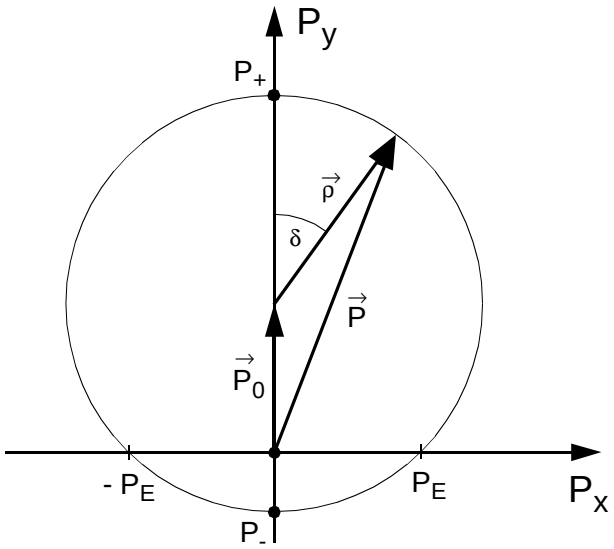


**Figure 3.** *A circular Coulomb orbit in momentum space ('Hodograph').*

are constant in time [9, 10] (see figure 3, where the $p_z$–axis has been chosen along $\vec{L}$ and the $p_y$–axis in the direction of $\vec{p}_0$ ). This circular orbit in momentum space is the 'hodograph', already described by Hamilton (see the references given in [9, 10]). The vector

$$\vec{\rho} = \vec{p} - \vec{p}_0 \tag{3.8}$$

moves along the circle (3.5) according to

$$\begin{aligned} \dot{\vec{\rho}} = \dot{\vec{p}} &= -\frac{c}{r^2}\,\hat{r} = -\frac{1}{mr^2}\left(\vec{p}\times\vec{L} - \vec{A}\right) \\ &= -\frac{1}{mr^2}\left((\vec{\rho}+\vec{p}_0)\times\vec{L} - \vec{A}\right) = -\frac{1}{mr^2}\,\vec{\rho}\times\vec{L} \end{aligned} \tag{3.9}$$

with $\vec{p}_0 \times \vec{L} = (\hat{L}\times\vec{A})\times\hat{L} = \vec{A}$ because $\vec{A}$ and $\vec{L}$ are orthogonal. This yields the equation

$$\dot{\vec{\rho}} = \vec{\omega}\times\vec{\rho} \tag{3.10}$$

for the motion along the momentum circle with (time-dependent) frequency

$$\vec{\omega} = \frac{\vec{L}}{mr^2}\,. \tag{3.11}$$

The angular velocity is maximum/minimum at the maximum/minimum value of the momentum

$$p_\pm = \rho \pm p_0\,. \tag{3.12}$$

Introducing the abbreviation

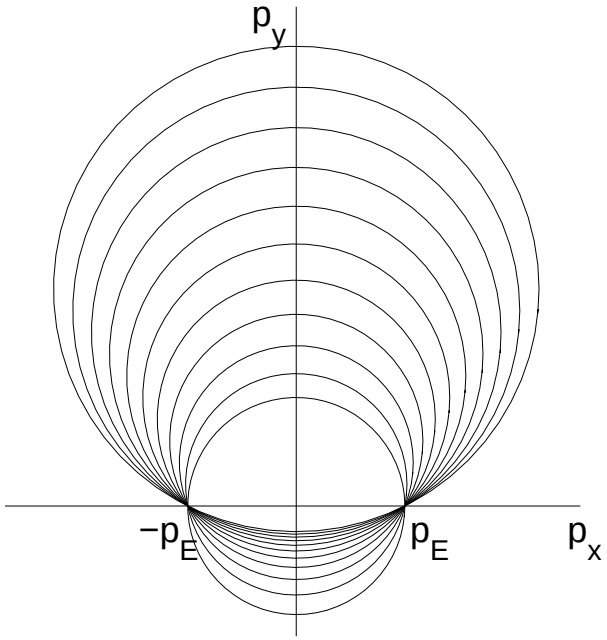


**Figure 4.** *Momentum space orbits for the Coulomb potential.*

$$p_E^2 = -2mE = \rho^2 - p_0^2 = p_+ p_- \tag{3.13}$$

we see that all coplanar momentum space orbits oriented in the same way (i.e. same $\hat{L}$ and $\hat{A}$) with the same energy pass through the points $p_y = 0$ and $p_x = \pm p_E$, as shown in figure 4. The magnitude of the momentum $p = |\vec{p}|$ is restricted to the classically allowed region $p_- \le p \le p_+$ , where the boundaries $p_\pm$ depend on the angular momentum. For the maximum accessible value $L = L_{\max} = cm/p_{\rm E}$ this region shrinks to zero: $p = p_- = p_+ = p_{\rm E}$, i.e. the absolute value of the momentum is constant. This is, of course, immediately clear from the virial theorem, which states for the Coulomb potential that the average total energy ($= -p_{\rm E}^2/2m$) equals the negative average kinetic energy ($=-p^2/2m$ for a circular orbit in position space). In the limit $L \to 0$ (a free–fall orbit), $p_-$ approaches zero and $p_+$ goes to infinity. The geometric properties of the momentum space trajectories are investigated very extensively (although quite different to our approach) in [11].

We are now interested in the probability distribution $w_{E,L}(p)$ of the momentum $p$ for a given value of the energy $E$ and the angular momentum $L$. Following equation (2.8) in [1] we have

$$w_{E,L}(p) = \frac{2}{T|\dot{p}|} = \frac{2p}{T|\vec{p}\cdot\dot{\vec{p}}|} = \frac{2p}{T|\vec{p}\cdot\dot{\vec{\rho}}|} \tag{3.14}$$

(again, the factor 2 arises from the fact that along the orbit each value of $p$ appears

twice with equal probability). The denominator can be written as

$$\begin{aligned}\vec{p}\cdot\dot{\vec{\rho}} &= \vec{p}\cdot(\vec{\omega}\times\vec{\rho}) = (\vec{\rho}+\vec{p}_0)\cdot(\vec{\omega}\times\vec{\rho}) \\ &= \vec{p}_0\cdot(\vec{\omega}\times\vec{\rho}) = \vec{\omega}\cdot(\vec{\rho}\times\vec{p}_0) = \omega\rho\, p_0 \sin\delta\,,\end{aligned} \tag{3.15}$$

where $\delta$ is the angle between $\vec{\rho}$ and $\vec{p}_0$ (see figure 3). Here we can distinguish a geometric factor resulting from the projection of the circle and a time factor given by the variation of the angular velocity along the momentum circle, given by

$$\omega = \frac{L}{4m^3c^2}\left(p^2+p_{\mathrm{E}}^2\right)^2. \tag{3.16}$$

Now it is an elementary task to rewrite $\sin\delta$ by $\cos\delta$, which can be obtained from $p^2 = \rho^2 + p_0^2 - 2\rho p_0\cos\delta$. After inserting $T$ given in (3.3) and $\omega$, we obtain

$$w_{E,L}(p) = \frac{8mcp_{\mathrm{E}}^3 p}{\pi L\left(p^2+p_E^2\right)^2\sqrt{4\rho^2p_0^2-(p^2-p_0^2-\rho^2)^2}}\,, \tag{3.17}$$

which can be rewritten in the more convenient form

$$w_{E,L}(p) = \frac{\lambda p}{\left(p_E^2+p^2\right)^2\sqrt{(p_+^2-p^2)(p^2-p_-^2)}} \tag{3.18}$$

with

$$\lambda = \frac{8mcp_{\mathrm{E}}^3}{\pi L}\,. \tag{3.19}$$

At the boundaries of the classical allowed regions, $p_\pm$, the distributions diverge.

One can easily check that this distribution is normalized and that $\langle p^2\rangle = p_{\mathrm{E}}^2$, as already known from the virial theorem. Three limiting distributions are of interest: For $L = L_{\max}$ the distribution shrinks to a point:

$$w_{E,L_{\max}} = \delta(p-p_{\mathrm{E}})\,. \tag{3.20}$$

For the free–fall orbit $L = 0$ we have

$$w_{E,0}(p) = \frac{4p_{\mathrm{E}}^3}{\left(p^2+p_{\mathrm{E}}^2\right)^2}\,. \tag{3.21}$$

If the value of the angular momentum $L$ is unknown (or not specified) we can average over all possible values and orientations of $\vec{L}$ in space, which is accounted for by a weight factor $L$. This leads to the micro-canonical momentum distribution [12]

$$\overline{w}_E(p) = \frac{\displaystyle\int_0^{L_{\max}} w_{E,L}(p)L\,\mathrm{d}L}{\displaystyle\int_0^{L_{\max}} L\,\mathrm{d}L} = \frac{32p_{\mathrm{E}}^5p^2}{\pi\left(p^2+p_{\mathrm{E}}^2\right)^4}\,, \tag{3.22}$$

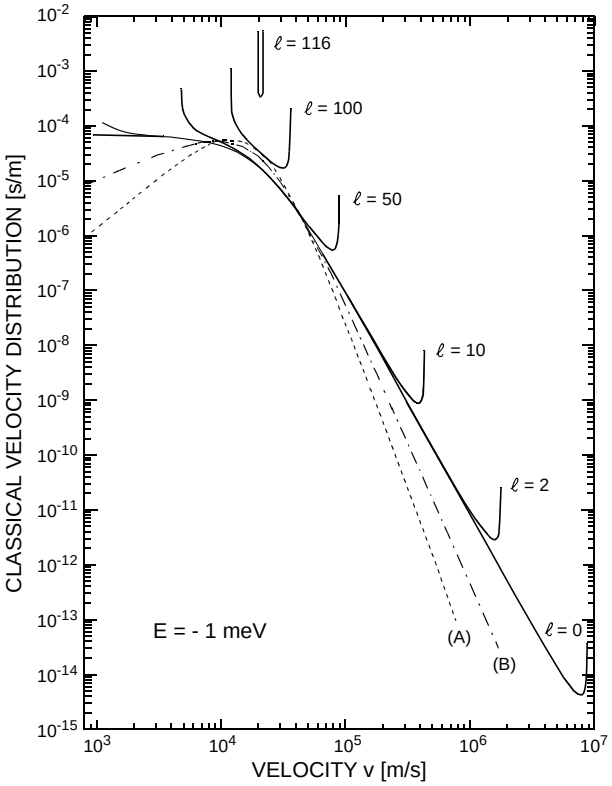


**Figure 5.** *Classical distributions of the velocity $v = p/m$ for a highly excited Hydrogen atom ($E = -1\,meV$) for various values of the angular momentum quantum number $\ell$ ($L = (\ell + 1/2)\hbar$) (taken from [13]).*

which can also be calculated directly by means of

$$\overline{w}_E(p) \sim \int \delta(p - p')\delta\Big(E - \frac{p'^2}{2m} + \frac{c}{r'}\Big)\, \mathrm{d}^3r'\, \mathrm{d}^3p' \,. \tag{3.23}$$

As an illustration, figure 5 (taken from [13]) shows the classical distributions of the velocity $v = p/m$ for a highly excited Hydrogen atom ($E = -1\,\mathrm{meV}$) for various values of the angular momentum quantum number $\ell$ ($L = (\ell + 1/2)\hbar$, [14]). With increasing $\ell$, the distributions change from the free fall distribution (3.21) to the localized distribution (3.20) for a circular orbit in position space. Also shown is the $L$–averaged micro-canonical distribution (3.22) (A) as well as a two–dimensional average (B). In the double–logarithmic plot one observes the power–law decay at high momenta according to $\sim p^{-(d+3)}$ for $d = 1, 2$ and 3 dimensions.

The semiclassical momentum distributions for the Coulomb potentials for fixed values of $E$ and $\ell$ can be obtained in the same manners as described in section 2.3 of [1]. Here, however, the two contributions — the two intersections with the momentum space circle (3.5) with the circle $|\vec{p}| = p$ — appear with the same weight, simply because of symmetry, exactly as for the well–known case of the one-dimensional position distributions. The semiclassical interference between these two contributions is given

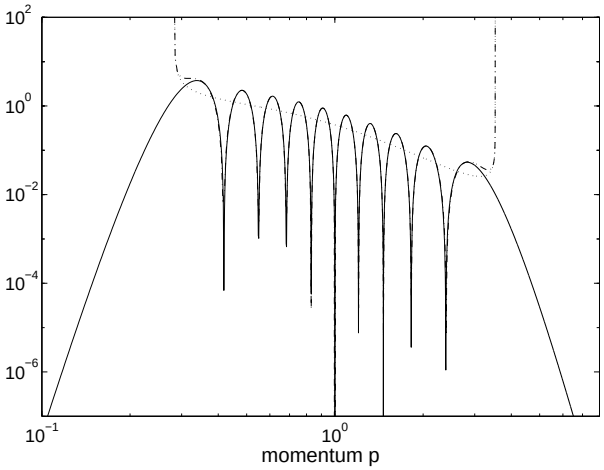


**Figure 6.** *Quantum (—), classical (· · ·) and semiclassical (– · –·) momentum distributions for the state $n = 4$, $l = 10$ of the Coulomb potential.*

by the action integral

$$S(p) = \int_{r_-}^{r_{E,L}(p)} p_{E,L}(r')\mathrm{d}r' - \sqrt{(p\, r_{E,L}(p))^2 - L^2} + L \arccos\left(\frac{L}{p\, r_{E,L}(p)}\right) \tag{3.24}$$

with $p_{E,L}(r) = \pm\sqrt{2m(E + c/r) - L^2/r^2}$ and $r_{E,L}(p)$ given by inversion of this formula. We need the difference between the action calculated on the two branches, which can be written in closed form

$$\begin{aligned}\Delta S(p) = &- \ell \arcsin \frac{1 - \frac{\ell^2}{2n^2}(u^2-1)}{\sqrt{1-\ell^2/n^2}} - \ell \arcsin \frac{\ell(u^2+1)}{2nu} \\ &- n \arcsin \frac{u^2-1}{(u^2+1)\sqrt{1-\ell^2/n^2}} + (\ell + n/2)\pi\,,\end{aligned} \tag{3.25}$$

with $L = (\ell + 1/2)\hbar$ and $u = p/p_{\mathrm{E}}$. The final result for the semiclassical momentum distribution is

$$\left|\psi^{\mathrm{sc}}_{n,\ell}(p)\right|^2 = 2w_{E,L}\cos(\Delta S(p) + \pi/4). \tag{3.26}$$

The exact quantum momentum distribution is given by [15] (see also [16])

$$\psi^{\mathrm{qm}}_{n,\ell}(p) = \sqrt{\frac{2}{\pi}\frac{(n-\ell-1)!}{(n+l)!}}\, n^2 2^{2(\ell+1)}\ell! \frac{n^\ell p^\ell}{(n^2p^2+1)^{\ell+2}}\, C^{\ell+1}_{n-\ell-1}\left(\frac{n^2p^2-1}{n^2p^2+1}\right) \tag{3.27}$$

$(0 \le \ell \le n-1)$, where the $C^k_m(x)$ are the Gegenbauer polynomials.

Figures 6 and 7 show a comparison between the quantum, classical and semiclassical Coulomb momentum distributions for the quantum states $n = 20$ and $\ell = 0$ or $\ell = 10$, respectively, again in a double–logarithmic plot. The $n - \ell - 1$ nodes of the momentum

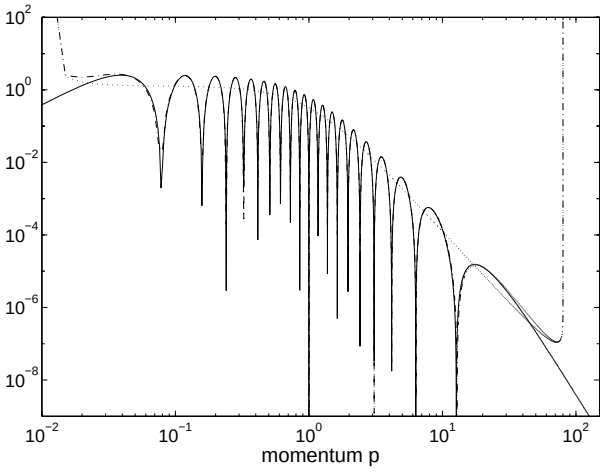


**Figure 7.** *Same as figure 6, but* $l = 0$.

space wavefunction are (almost) precisely reproduced by the semiclassical formula, which, of course, still shows the divergence at the classical boundaries.

It is interesting to observe that the $\ell$-averaged quantum distribution

$$\overline{w_n}^{qm}(p) = \frac{1}{n^2}\sum_{\ell=0}^{n-1}(2\ell+1)|\Psi_{n,\ell}^{qm}(p)|^2 \tag{3.28}$$

which can be evaluated analytically [17] agrees *precisely* with the purely classical formula (3.22) at the bound state energy $E_n = -mc^2/(2\hbar^2 n^2)$ [13]. This appears to be a manifestation of the correspondence identities, as, e.g., the Rutherford scattering identity, the Bohr–Sommerfeld identity or the Fock identity, where the last one is a special case of the above shown momentum space distribution functions. These so–called correspondence identities are investigated in [18] for the hydrogen atom and in [19] for general cases.

It should be noted that quantum momentum distributions also show up in Coulomb scattering applications. A discussion of the quantum and semiclassical (off-shell) $T$ Matrix in momentum space can be found, e.g., in reference [20]. Finally, we would like to point out that the momentum space representation is also directly related to experimentally observable properties, as for example ionization and attachment processes in hydrogenic atoms [13] or collision induced dissociation of molecules [4].

## 4. Summary

In continuation of [1], where the general theory was given, we discussed the Morse oscillator and the Coulomb potential. This discussion may help to improve the knowledge on the basic properties of momentum space representations together with the well-known one in position space. New insight to the understanding of systems can be gained by considering *both* representations. To achieve this goal, considering

(semi-)classical wavefunctions may be very useful, even if it is possible to calculate the quantum wavefunctions. It is demonstrated, that computing wavefunctions by a (nonuniform) semiclassical theory at least in the classical allowed phase space regions is straightforward.

## References


[1] H. J. Korsch and B. Schellhaaß, *Quantum, classical and semiclassical momentum distributions. I. Theory and elementary examples*, Eur. J. Phys. **xxx** (1999) xxx, in press

[2] S. Flügge, *Practical Quantum Mechanics*, Springer, Berlin, 1974

[3] M. Abramowitz and I. A. Stegun, *Handbook of Mathematical Functions*, Dover Publications, Inc., New York, New York, 1972

[4] P. Eckelt and H. J. Korsch, *Collision–Induced Dissociation: Differential Energy Transfer Probabilities*, Chem. Phys. Lett. **18** (1973) 584

[5] J. P. Dahl and M. Springborg, *The Morse oscillator in position space, momentum space, and phase space*, J. Chem. Phys. **88** (1988) 4535

[6] L. J. Slater, *Confluent Hypergeometric Functions*, Cambridge Univ. Press, London, 1960

[7] S. W. Benson and C. C. Behrend, *Vibrational Energy Exchange of Highly Excited Anharmonic Oscillators*, J. Chem. Phys. **40** (1964) 1289

[8] M. C. Gutzwiller, *Chaos in Classical and Quantum Mechanics*, Springer, New York, 1990

[9] H. Goldstein, *Prehistory of the "Runge-Lenz" vector*, Am. J. Phys. **43** (1975) 737

[10] H. Goldstein, *More on the prehistory of the Laplace or Runge-Lenz vector*, Am. J. Phys. **44** (1976) 1123

[11] M. C. Gutzwiller, *Phase-Integral Approximation in Momentum Space and the Bound States of an Atom. II*, J. Math. Phys. **10(6)** (1969) 1004

[12] M. Gryziński, *Probalistic description of the electron motion in the Coulomb field of nucleus*, J. Physique **43** (1982) L–425

[13] D. Klar, B. Mirbach, H. J. Korsch, M. W. Ruf, and H. Hotop, *Comparison of rates for Rydberg electron attachment with those for free electron attachment*, Z. Phys. D **31** (1994) 235

[14] M. Robnik and L. Salasnich, *WKB expansion for the angular momentum and the Kepler problem: from the torus quantization to the exact one*, J. Phys. A **30** (1997) 1719

[15] H. A. Bethe and E. E. Salpeter, *Quantum mechanics of one- and two-electron atoms*, Springer, 1957

[16] J. S. Briggs and L. Dubé, *The second Born approximation to the electron transfer cross section*, J. Phys. B **13** (1980) 771

[17] R. M. May, *Sum Rules for Hydrogenic Wave Functions, with Applications to Charge-Exchange and Ionization Processes*, Phys. Rev. **136(3A)** (1964) A669

[18] A. Norcliffe and I. C. Percival, *Correspondence identities II. The Bohr – Sommerfeld identity for the hydrogen atom*, J. Phys. B **1** (1968) 784

[19] A. Norcliffe and I. C. Percival, *Correspondence identities: I*, J. Phys. B **1** (1968) 774

[20] H. J. Korsch and R. Möhlenkamp, *Off–Shell T Matrix in the Semiclassical Limit*, J. Phys. B **15** (1982) 2187